Absorption Spectra of CuGaSe 2 and CuInSe 2 Semiconducting Nanoclusters

ARTICLE *in* THE JOURNAL OF PHYSICAL CHEMISTRY C · SEPTEMBER 2015

Impact Factor: 4.77 · DOI: 10.1021/acs.jpcc.5b07350

3 AUTHORS, INCLUDING:

Junais Mokkath

National Institute for Materials Science

13 PUBLICATIONS **45** CITATIONS

SEE PROFILE

Nirpendra Singh

King Abdullah University of Science and Techn…

44 PUBLICATIONS **302** CITATIONS

SEE PROFILE

THE JOURNAL OF PHYSICAL CHEMISTRY C

Article

pubs.acs.org/JPCC

Absorption Spectra of $CuGaSe_2$ and $CuInSe_2$ Semiconducting Nanoclusters

Junais Habeeb Mokkath, Nirpendra Singh, and U. Schwingenschlögl*

Physical Science & Engineering Division, KAUST, Thuwal 23955-6900, Kingdom of Saudi Arabia

Supporting Information

ABSTRACT: The structural and optical properties of the chalcopyrite $Cu_nGa_nSe_{2n}$ and $Cu_nIn_nSe_{2n}$ nanoclusters (n = 2, 4, 6, and 8) are investigated as a function of the size using a combination of basin-hopping global optimization and time-dependent density functional theory. Although the lowest energy structures are found to show almost random geometries, the band gaps and absorption spectra still are subject to systematic blue shifts for decreasing cluster size in the case of $Cu_nGa_nSe_{2n}$, indicating strong electron confinement. The applicability of the nanoclusters in photovoltaics is discussed.

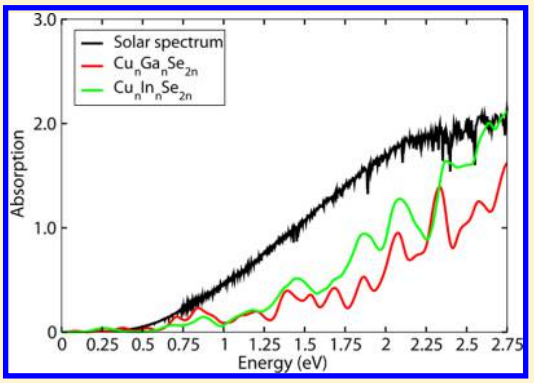

I. INTRODUCTION

Semiconductor nanocrystals have been used in photovoltaics as active absorber layer[1,2] and as ink for solution-processed solar cells.[3] They are capable of absorbing a large fraction of the solar spectrum because the band gaps are modified by quantum confinement.[4] Thin films of $CuGaSe_2$, $CuInSe_2$, and $Cu(Ga,In)Se_2$ have been studied for more than two decades as p-type semiconductors for light harvesting,[5] achieving an efficiency of 20%;[6,7] however, a critical issue of thin-film solar cells is the reduced absorption due to the small thickness. Guo and coworkers have prepared solar cells on Mo-coated soda lime glass using $CuInSe_2$ nanocrystal ink and the drop cast method, achieving an efficiency of 3.2%,[8] while Panthani and coworkers have used diphenylphosphine selenide as precursor.[9]

$Cu(Ga,In)Se_2$ nanocrystals have been synthesized by the authors of refs 10 and 11. In ref 11, a phosphine-free scalable process has been used and a strong composition dependence of the optical absorption with band gaps from 1.48 to 2.10 eV has been demonstrated. Nanoclusters with sizes from 1.2 to 5.6 nm can be obtained by colloidal routes.[12] In general, the synthesis of ultrasmall nanoclusters of uniform size poses huge experimental problems below the exciton Bohr radius, which is 10.6 nm in bulk $CuInSe_2$, for example.[13] Thermal decomposition,[14] solid-state reactions,[15] and solvothermal methods[16] have been used to characterize the nanoclusters. Oriented films of self-assembled $CuInSe_2$ nanoclusters have been demonstrated in ref 17. In general, in nanoclusters the exciton is spatially confined, which has important effects on the optical properties, including increasing band gaps and exciton energies as well as blue shifts of the absorption spectra.[18] Bulk $Cu(Ga,In)Se_2$ has been analyzed in great detail by theoretical methods,[19−23] whereas nanoclusters have not been touched, despite promising experimental data.[8,10] Specifically, the influence of the nanocluster size on the structure and absorption properties is not understood.

II. COMPUTATIONAL ASPECTS

Initial topologies of the $Cu_nGa_nSe_{2n}$ and $Cu_nIn_nSe_{2n}$ (n = 2, 4, 6, and 8) nanoclusters are generated using a cluster graph approach.[24,25] Determining the structure of a nanoalloy cluster in general is a difficult computational problem, especially at the first-principles level.[26−31] One possible approach is the combination of global optimization by the genetic algorithm with density functional theory.[32] In the present study the problem is addressed by basin-hopping global optimization[33] with quantum Sutton-Chen[34] potentials as implemented in the EON code.[35] In short, this technique explores a transformed rather than the original potential energy surface, which is obtained by mapping onto a set of interpenetrating staircases with plateaus corresponding to each basin of attraction. We restrict the sampling to atomic moves (maximal distance of 0.6) and exchange (probability of 0.5). A Gaussian displacement distribution is employed as well as a conjugate gradient optimization. For each size we perform basin-hopping runs of ∼20 000 with a low thermal energy of 0.2 eV. We have tested that increasing the thermal energy to 0.3 eV does not affect the lowest energy structures.

The lowest energy structures obtained from basin-hopping global optimization are reoptimized by density functional theory to achieve a high accuracy, using the NWCHEM package[36] with the B3LYP[37] exchange correlation functional and the CRENBL basis set and effective core potentials.[38] The

Received: July 30, 2015
Revised: September 7, 2015
Published: September 21, 2015

DOI: 10.1021/acs.jpcc.5b07350
J. Phys. Chem. C 2015, 119, 22732−22736

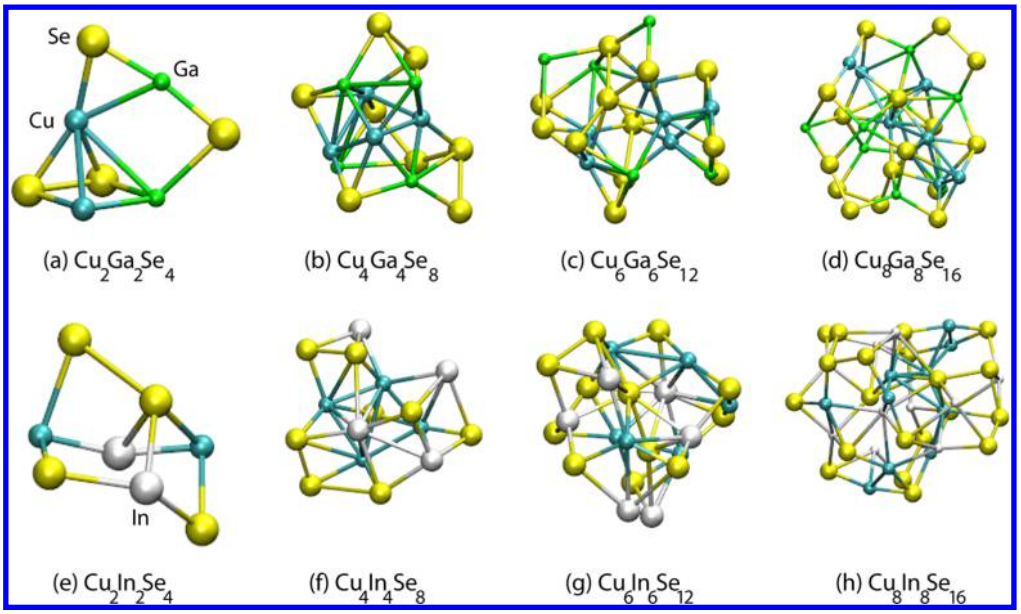

Figure 1. Lowest energy structures of the $Cu_nGa_nSe_{2n}$ and $Cu_nIn_nSe_{2n}$ nanoclusters (n = 2, 4, 6, and 8).

B3LYP functional improves the description of the band gap by inclusion of Hartree−Fock exchange. The optimization is assumed to be converged when the energies and atomic displacements have declined below thresholds of 10^{-4} eV and 5×10^{-3} Å. We have also reoptimized all structures that are up to 1 eV higher in energy than the favorable structures after basin-hopping global optimization and find that they stay clearly above the energy minimum. Moreover, we have checked by phonon calculations that the obtained structures (Cartesian coordinates given in the Supporting Information) correspond to minima on the potential energy surface. The relation between the interatomic potential energy and the energy obtained from density functional theory is demonstrated in Figure S1 in the Supporting Information. The lowest energy reoptimized structures are studied by optical calculations within time-dependent density functional theory,[39] using the same basis set and exchange correlation functional as in the static calculations, which gives a reliable description of the excitation spectra of a wide range of systems.[40−42] To this aim, we use the Kohn-Shan eigenvalues and orbitals from the static calculations and employ the linear response technique.[43] The NWCHEM implementation of the linear response technique makes use of the Tamm-Dancoff approximation,[44] which assumes that off-diagonal matrix elements are negligible. The number of roots to be extracted is critical for the required computation time but must be chosen sufficiently high as it controls the upper limit of the spectrum. The following results are based on 100 roots.

III. RESULTS AND DISCUSSION

The lowest energy structures of the $Cu_nGa_nSe_{2n}$ and $Cu_nIn_nSe_{2n}$ nanoclusters are shown in Figure 1 for n = 2, 4, 6, and 8. All are low-symmetry structures, reflecting the fact that even the bulk compounds show significant structural distortions and variations in the local atomic arrangements.[45] We have also performed basin-hopping optimizations using as initial topologies fragments of the bulk compounds; however, these topologies are found to relax always to high-energy structures. Figure 1 shows a large structural variety, but there remain some systematics in the atomic bonding. The Se atoms tend toward the surface and the Cu atoms toward the core of the nanocluster, although a clear classification into surface and core regions is difficult. These preferences can be explained on the basis of the bulk cohesive energies and surface energies of Cu, Ga, In, and Se. The bulk cohesive energies fulfill the relation Cu (3.49 eV) > Ga (2.81 eV) > In (2.52 eV) > Se (2.46 eV), which suggests that the Cu atoms favor the core to increase the number of Cu−Cu bonds. Surface segregation of Se is energetically favorable because the surface energies follow the series Cu (1.79 Jm^{-2}) > Ga (1.11 Jm^{-2}) > In (0.68 Jm^{-2}) > Se (0.29 Jm^{-2}).[46] The small atomic radius of Se as compared with that of Cu (1.28 Å), Ga (1.41 Å), In (1.66 Å), and Se (1.14 Å)[47] supports this trend.

Table 1 gives the energy gap between the highest occupied molecular orbital (HOMO) and the lowest unoccupied molecular orbital (LUMO) as well as the optical gap for each nanocluster. While the HOMO−LUMO gap is a ground state property, the optical gap is the energy difference between the ground state and first excited state. For all of the investigated nanoclusters the optical gap is consistently smaller than the HOMO−LUMO gap because of strong excitonic effects as a consequence of the spatial confinement. An important role of excitons previously also has been reported for bulk $CuGaSe_2$[21] and bulk $CuInSe_2$.[48] According to Figure 2, for all of the studied nanoclusters the HOMO, LUMO, and nearby states are dominated by the Se 4p orbitals. Figure 2 also shows small shifts of the HOMO and substantial shifts of the LUMO as a function of the nanocluster size for both $Cu_nGa_nSe_{2n}$ and $Cu_nIn_nSe_{2n}$. A similar behavior has been found in bulk $CuGaSe_2$ using near-edge X-ray absorption fine structure spectroscopy.[49]

The absorption spectra of the lowest energy structures in Figure 3 show rich features and significant variations as a function of the nanocluster size. We find systematic blue shifts for decreasing size in the case of $Cu_nGa_nSe_{2n}$, reflecting quantum confinement. Beyond the blue shifts, even the addition of only few atoms turns out to have huge effects on the spectra. The absorption spectrum of $Cu_2Ga_2Se_4$ is characterized by two pronounced peaks at 2.3 and 2.7 eV. The first peak is due to the transitions HOMO−1→ LUMO (70%), HOMO−1→ LUMO+1 (20%), and HOMO→ LUMO (10%), whereas the second peak is due to the transitions

DOI: 10.1021/acs.jpcc.5b07350
J. Phys. Chem. C 2015, 119, 22732−22736

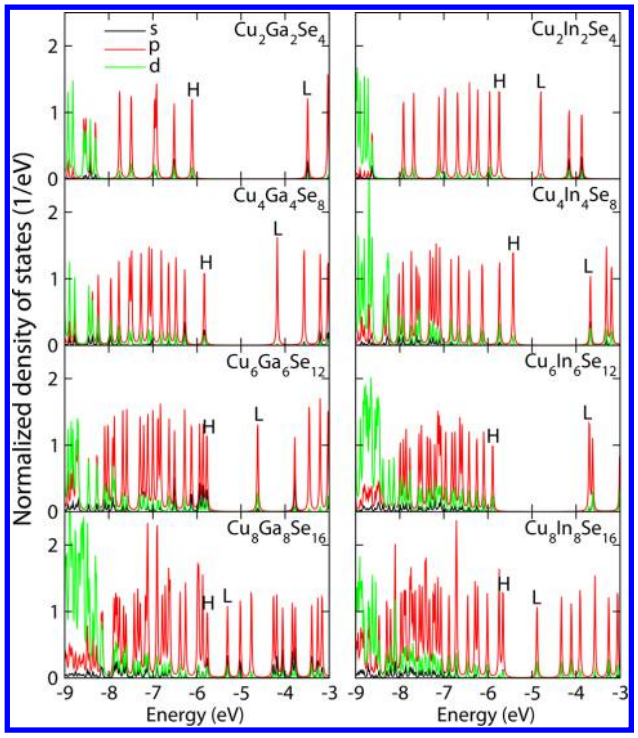

Figure 2. Density of states of the $Cu_nGa_nSe_{2n}$ and $Cu_nIn_nSe_{2n}$ nanoclusters. H and L represent the HOMO and LUMO, respectively.

HOMO−2→ LUMO (65%), HOMO−3→ LUMO+1 (20%), and HOMO→ LUMO+3 (15%). The involved orbitals are shown in Figure S2 in the Supporting Information. The absorption spectrum of the next larger nanocluster ($Cu_4Ga_4Se_8$) is still characterized by two pronounced peaks at 2.3 and 2.8 eV but with contributions from very different transitions. The first peak is due to the transitions HOMO→ LUMO+5 (64%), HOMO→ LUMO+4 (20%), and HOMO→ LUMO+3 (16%), whereas the second peak is due to the transitions HOMO−1→ LUMO+5 (65%), HOMO−2→ LUMO+2 (25%), and HOMO−5→ LUMO+2 (10%). The involved orbitals are shown in Figure S3 in the Supporting Information. For the other nanoclusters under investigation we find similar effects: Even when the spectra appear to be related, the underlying transitions vary strongly, reflecting the large structural differences from one nanocluster to the other.

As a common trend, we notice that the absorption spectra lose structure (the absorption peaks are less pronounced) when the nanocluster size increases, which applies to both $Cu_nGa_nSe_{2n}$ and $Cu_nIn_nSe_{2n}$. Still, as a general rule, we have to realize that the properties of a specific nanocluster are largely unpredictable. The absorption spectra of the nanoclusters under investigation also show hardly any agreement with the spectra of $CuGaSe_2$[51] and CuInSe2[52] thin films, which is to be expected from their special geometries. On the contrary, our results indicate that the concerted properties of a mixture of ultrasmall nanoclusters can be very useful. We plot in Figure 4 the average of the absorption spectra shown in Figure 3 for both $Cu_nGa_nSe_{2n}$ and $Cu_nIn_nSe_{2n}$. Comparison with the solar spectrum reveals an excellent overlap of the absorption range and therefore potential of application in photovoltaics.

IV. CONCLUSIONS

The structure and optical properties of the chalcopyrite $Cu_nGa_nSe_{2n}$ and $Cu_nIn_nSe_{2n}$ nanoclusters are found to show dramatic differences as a function of the nanocluster size. The lowest energy structures are characterized by almost random geometries without symmetry. The only clear structural trend is the affinity of Se toward the surface and of Cu toward the core of the nanocluster, in accordance with the cohesive energies, surface energies, and atomic radii of the bulk compounds. Despite very different structures, the absorption spectra still show systematic blue shifts for decreasing nanocluster size in the case of $Cu_nGa_nSe_{2n}$, pointing to strong electron confinement. The simultaneous presence of different sizes of nanoclusters broadens the absorption range to match well with the solar spectrum.

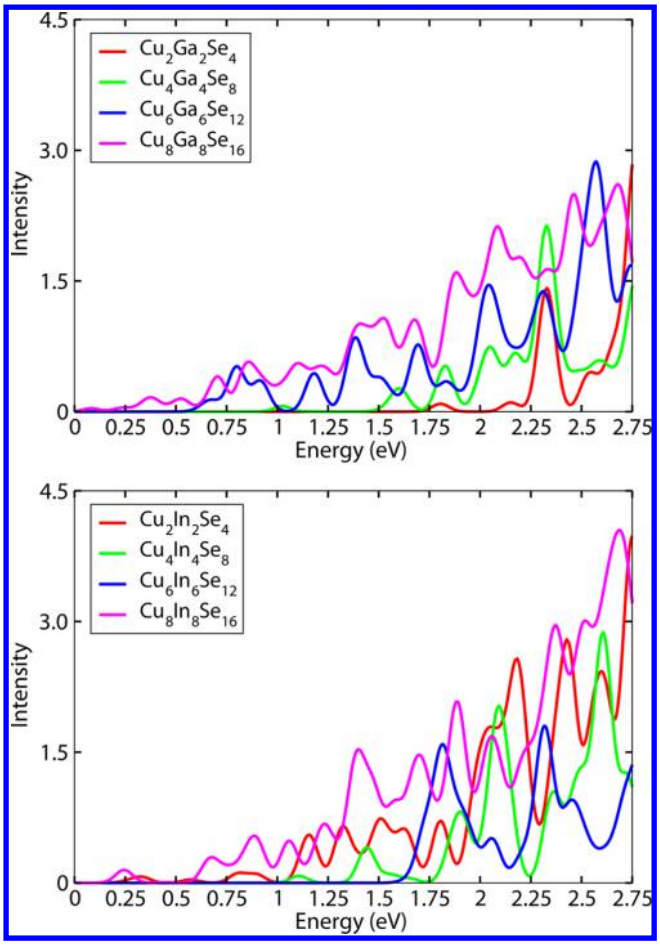

Figure 3. Optical absorption spectra of the $Cu_nGa_nSe_{2n}$ and $Cu_nIn_nSe_{2n}$ nanoclusters. A Gaussian width of 0.1 eV is used for broadening. The spectra are normalized with respect to the number of atoms.

Table 1. HOMO-LUMO and Optical Gaps of the $Cu_nGa_nSe_{2n}$ and $Cu_nIn_nSe_{2n}$ Nanoclusters

nanocluster	HOMO−LUMO gap (eV)	optical gap (eV)
$Cu_2Ga_2Se_4$	2.62	1.80
$Cu_4Ga_4Se_8$	1.65	1.02
$Cu_6Ga_6Se_{12}$	1.13	0.63
$Cu_8Ga_8Se_{16}$	0.47	0.12
$Cu_2In_2Se_4$	0.94	0.26
$Cu_4In_4Se_8$	1.75	1.11
$Cu_6In_6Se_{12}$	2.19	1.64
$Cu_8In_8Se_{16}$	0.77	0.24

DOI: 10.1021/acs.jpcc.5b07350
J. Phys. Chem. C 2015, 119, 22732−22736

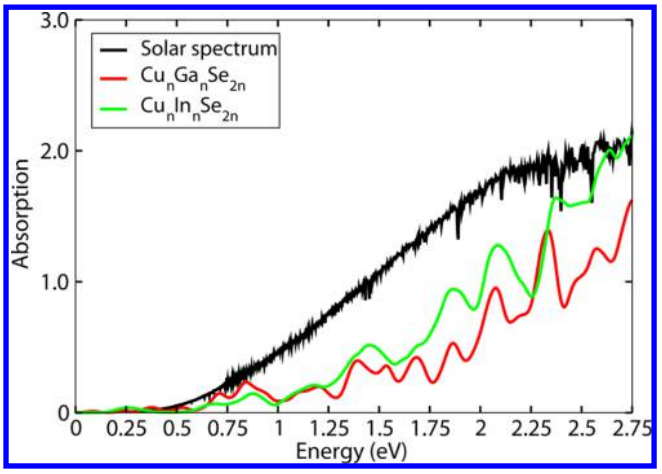

Figure 4. Comparison of size-averaged $Cu_nGa_nSe_{2n}$ and $Cu_nIn_nSe_{2n}$ optical absorption spectra with the solar spectrum.[50]

■ ASSOCIATED CONTENT

Supporting Information

The Supporting Information is available free of charge on the ACS Publications website at DOI: 10.1021/acs.jpcc.5b07350.

Atomic coordinates of the DFT optimized structures. Interatomic potential energy versus DFT energy. Orbitals involved in the absorption of the $Cu_2Ga_2Se_4$ nanocluster. Orbitals involved in the absorption of the $Cu_4Ga_4Se_8$ nanocluster. (PDF)

■ AUTHOR INFORMATION

Corresponding Author

*E-mail: udo.schwingenschlogl@kaust.edu.sa. Tel: +966(0) 544700080.

Notes

The authors declare no competing financial interest.

■ ACKNOWLEDGMENTS

Research reported in this publication was supported by the King Abdullah University of Science and Technology (KAUST). Computational resources provided by KAUST IT are gratefully acknowledged.

■ REFERENCES

(1) Gur, I.; Fromer, N. A.; Geier, M. L.; Alivisatos, A. P. Air-Stable All-Inorganic Nanocrystal Solar Cells Processed from Solution. *Science* **2005**, *310*, 462−465.

(2) Kamat, P. V. Quantum Dot Solar Cells. Semiconductor Nanocrystals as Light Harvesters. *J. Phys. Chem. C* **2008**, *112*, 18737−18753.

(3) Jasieniak, J.; MacDonald, B. I.; Watkins, S. E. Solution-Processed Sintered Nanocrystal Solar Cells via Layer-by-Layer Assembly, Mulvaney, P. *Nano Lett.* **2011**, *11*, 2856−2864.

(4) Brus, L. E. Electron-Electron and Electron-Hole Interactions in Small Semiconductor Crystallites: The Size Dependence of the Lowest Excited Electronic State. *J. Chem. Phys.* **1984**, *80*, 4403−4409.

(5) Niki, S.; Contreras, M.; Repins, I.; Powalla, M.; Kushiya, K.; Ishizuka, S.; Matsubara, K. CIGS Absorbers and Processes. *Prog. Photovoltaics* **2010**, *18*, 453−466.

(6) Repins, I.; Contreras, M. A.; Egaas, B.; DeHart, C.; Scharf, J.; Perkins, C. L.; TO, B.; Noufi, R. 19.9%-Efficient ZnO/CdS/$CuInGaSe_2$ Solar Cell with 81.2% Fill Factor. *Prog. Photovoltaics* **2008**, *16*, 235−239.

(7) Jackson, P.; Hariskos, D.; Lotter, E.; Paetel, S.; Wuerz, R.; Menner, R.; Wischmann, W.; Powalla, M. New World Record Efficiency for $Cu(In,Ga)Se_2$ Thin-Film Solar Cells beyond 20%. *Prog. Photovoltaics* **2011**, *19*, 894−897.

(8) Guo, Q. J.; Kim, S. J.; Kar, M.; Shafarman, W. N.; Birkmire, R. W.; Stach, E. A.; Agrawal, R.; Hillhouse, H. W. Development of $CuInSe_2$ Nanocrystal and Nanoring Inks for Low-Cost Solar Cells. *Nano Lett.* **2008**, *8*, 2982−2987.

(9) Panthani, M. G.; Stolle, C. J.; Reid, D. K.; Rhee, D. J.; Harvey, T. B.; Akhavan, V. A.; Yu, Y.; Korgel, B. A. $CuInSe_2$ Quantum Dot Solar Cells with High Open-Circuit Voltage. *J. Phys. Chem. Lett.* **2013**, *4*, 2030−2034.

(10) Tang, J.; Hinds, S.; Kelley, S. O.; Sargent, E. H. Synthesis of Colloidal $CuGaSe_2$, $CuInSe_2$, and $Cu(InGa)Se_2$ Nanoparticles. *Chem. Mater.* **2008**, *20*, 6906−6910.

(11) Dilena, E.; Xie, Y.; Brescia, R.; Prato, M.; Maserati, L.; Krahne, R.; Paolella, A.; Bertoni, G.; Povia, M.; Moreels, I.; Manna, L. $CuIn_xGa_{1-x}S_2$ Nanocrystals with Tunable Composition and Band Gap Synthesized via a Phosphine-Free and Scalable Procedure. *Chem. Mater.* **2013**, *25*, 3180−3187.

(12) Nose, K.; Omata, T.; Otsuka-Yao-Matsuo, S. Colloidal Synthesis of Ternary Copper Indium Diselenide Quantum Dots and their Optical Properties. *J. Phys. Chem. C* **2009**, *113*, 3455−3460.

(13) Zhong, H.; Wang, Z.; Bovero, E.; Lu, Z.; van Veggel, F. C. J. M.; Scholes, G. D. Colloidal $CuInSe_2$ Nanocrystals in the Quantum Confinement Regime: Synthesis, Optical Properties, and Electroluminescence. *J. Phys. Chem. C* **2011**, *115*, 12396−12402.

(14) Castro, S. L.; Bailey, S. G.; Raffaelle, R. P.; Banger, K. K.; Hepp, A. F. Nanocrystalline Chalcopyrite Materials ($CuInS_2$ and $CuInSe_2$) via Low-Temperature Pyrolysis of Molecular Single-Source Precursors. *Chem. Mater.* **2003**, *15*, 3142−3147.

(15) Schoen, D. T.; Peng, H.; Cui, Y. Anisotropy of Chemical Transformation from In_2Se_3 to $CuInSe_2$ Nanowires through Solid State Reaction. *J. Am. Chem. Soc.* **2009**, *131*, 7973−7975.

(16) Li, B.; Xie, Y.; Huang, J.; Qian, Y. Synthesis by a Solvothermal Route and Characterization of $CuInSe_2$ Nanowhiskers and Nanoparticles. *Adv. Mater.* **1999**, *11*, 1456−1459.

(17) Reifsnyder, D. C.; Ye, X.; Gordon, T. R.; Song, C.; Murray, C. B. Three-Dimensional Self-Assembly of Chalcopyrite Copper Indium Diselenide Nanocrystals into Oriented Films. *ACS Nano* **2013**, *7*, 4307−4315.

(18) Bera, D.; Qian, L.; Tseng, T.-K.; Holloway, P. H. Quantum Dots and Their Multimodal Applications: A Review. *Materials* **2010**, *3*, 2260−2345.

(19) Ludwig, C. D. R.; Gruhn, T.; Felser, C.; Schilling, T.; Windeln, J.; Kratzer, P. Indium-Gallium Segregation in $CuIn_xGa_{1-x}Se_2$: An Ab Initio-Based Monte Carlo Study. *Phys. Rev. Lett.* **2010**, *105*, 025702.

(20) Vidal, J.; Botti, S.; Olsson, P.; Guillemoles, J.-F.; Reining, L. Strong Interplay between Structure and Electronic Properties in $CuIn(S,Se)_2$: A First-Principles Study. *Phys. Rev. Lett.* **2010**, *104*, 056401.

(21) Aguilera, I.; Vidal, J.; Wahnon, P.; Reining, L.; Botti, S. First-Principles Study of the Band Structure and Optical Absorption of $CuGaS_2$. *Phys. Rev. B: Condens. Matter Mater. Phys.* **2011**, *84*, 085145.

(22) Choi, S. G.; Chen, R.; Persson, C.; Kim, T. J.; Hwang, S. Y.; Kim, Y. D.; Mansfield, L. M. Dielectric Function Spectra at 40 K and Critical-Point Energies for $CuIn_{0.7}Ga_{0.3}Se_2$. *Appl. Phys. Lett.* **2012**, *101*, 261903.

(23) Azulay, D.; Balberg, I.; Millo, O. Microscopic Evidence for the Modification of the Electronic Structure at Grain Boundaries of $Cu(In_{1-x},Ga_x)Se_2$ Films. *Phys. Rev. Lett.* **2012**, *108*, 076603.

(24) Pastor, G. M.; Hirsch, R.; Mühlschlegel, B. Electron Correlations, Magnetism, and Structure of Small Clusters. *Phys. Rev. Lett.* **1994**, *72*, 3879−3882.

(25) Mokkath, J. H.; Pastor, G. M. First-Principles Study of Structural, Magnetic, and Electronic Properties of Small Fe-Rh Alloy Clusters. *Phys. Rev. B: Condens. Matter Mater. Phys.* **2012**, *85*, 054407.

DOI: 10.1021/acs.jpcc.5b07350
J. Phys. Chem. C 2015, 119, 22732−22736

(26) Jellinek, J.; Krissinel, E. B. Ni_nAl_m Alloy Clusters: Analysis of Structural Forms and Their Energy Ordering. *Chem. Phys. Lett.* **1996**, *258*, 283−292.
(27) Hamad, S.; Catlow, C. R. A.; Spano, E.; Matxain, J. M.; Ugalde, J. M. Structure and Properties of ZnS Nanoclusters. *J. Phys. Chem. B* **2005**, *109*, 2703−2709.
(28) Nguyen, K. A.; Day, P. N.; Pachter, R. Understanding Structural and Optical Properties of Nanoscale CdSe Magic-Size Quantum Dots: Insight from Computational Prediction. *J. Phys. Chem. C* **2010**, *114*, 16197−16209.
(29) Zwijnenburg, M. A. Optical Excitations in Stoichiometric Uncapped ZnS Nanostructures. *Nanoscale* **2011**, *3*, 3780−3787.
(30) Nguyen, K. A.; Pachter, R.; Day, P. N. Computational Prediction of Structures and Optical Excitations for Nanoscale Ultrasmall ZnS and CdSe Clusters. *J. Chem. Theory Comput.* **2013**, *9*, 3581−3596.
(31) Azpiroz, J. M.; Ugalde, J. M.; Infante, I. Benchmark Assessment of Density Functional Methods on Group II-VI MX (M = Zn, Cd; X = S, Se, Te) Quantum Dots. *J. Chem. Theory Comput.* **2014**, *10*, 76−89.
(32) Shayeghi, A.; Götz, D.; Davis, J. B. A.; Schäfer, R.; Johnston, R. L. Pool-BCGA: a Parallelised Generation-Free Genetic Algorithm for the Ab Initio Global Optimisation of Nanoalloy Clusters. *Phys. Chem. Chem. Phys.* **2015**, *17*, 2104−2112.
(33) Wales, D. J.; Doye, P. K. Global Optimization by Basin-Hopping and the Lowest Energy Structures of Lennard-Jones Clusters Containing up to 110 Atoms. *J. Phys. Chem. A* **1997**, *101*, 5111−5116.
(34) Qi, Y.; Cagin, T.; Kimura, Y.; Goddard, W. A. The Quantum Sutton-Chen Many-Body Potential for Properties of FCC Metals. *Phys. Rev. B: Condens. Matter Mater. Phys.* **1999**, *43*, 554.
(35) Basin Hopping—EON: Long Timescale Dynamics. http://theory.cm.utexas.edu/eon/basin_hopping.html.
(36) Valiev, M.; Bylaska, E. J.; Govind, N.; Kowalski, K.; Straatsma, T. P.; van Dam, H. J. J.; Wang, D.; Nieplocha, J.; Apra, E.; Windus, T. L.; de Jong, W. A. NWChem: A comprehensive and Scalable Open-Source Solution for Large Scale Molecular Simulations. *Comput. Phys. Commun.* **2010**, *181*, 1477−1489.
(37) Lee, C.; Yang, W.; Parr, R. G. Development of the Colle-Salvetti Correlation-Energy Formula into a Functional of the Electron Density. *Phys. Rev. B: Condens. Matter Mater. Phys.* **1988**, *37*, 785−789.
(38) LaJohn, L. A.; Christiansen, P. A.; Ross, R. B.; Atashroo, T.; Ermler, W. C. Ab Initio Relativistic Effective Potentials with Spin-Orbit Operators. III. Rb through Xe. *J. Chem. Phys.* **1987**, *87*, 2812−2824.
(39) Runge, E.; Gross, E. K. U. Density-Functional Theory for Time-Dependent Systems. *Phys. Rev. Lett.* **1984**, *52*, 997−1000.
(40) Barcaro, G.; Broyer, M.; Durante, N.; Fortunelli, A.; Stener, S. Alloying Effects on the Optical Properties of Ag-Au Nanoclusters from TDDFT Calculations. *J. Phys. Chem. C* **2011**, *115*, 24085−24091.
(41) Weissker, H.-C.; Mottet, C. Optical Properties of Pure and Core-Shell Noble-Metal Nanoclusters from TDDFT: The Influence of the Atomic Structure. *Phys. Rev. B: Condens. Matter Mater. Phys.* **2011**, *84*, 165443.
(42) Bae, G.-T.; Aikens, C. M. TDDFT and CIS Studies of Optical Properties of Dimers of Silver Tetrahedra. *J. Phys. Chem. A* **2012**, *116*, 8260−8269.
(43) Petersilka, M.; Gossmann, U. J.; Gross, E. K. U. Excitation Energies from Time-Dependent Density-Functional Theory. *Phys. Rev. Lett.* **1996**, *76*, 1212−1215.
(44) Hirata, S.; Head-Gordon, M. Time-Dependent Density Functional Theory Within the Tamm-Dancoff Approximation. *Chem. Phys. Lett.* **1999**, *314*, 291−299.
(45) Schnohr, C. S.; Kammer, H.; Stephan, C.; Schorr, S.; Steinbach, T.; Rensberg, J. Atomic-Scale Structure and Band-Gap Bowing in $Cu(In,Ga)Se_2$. *Phys. Rev. B: Condens. Matter Mater. Phys.* **2012**, *85*, 245204.
(46) Tyson, W. R.; Miller, W. A. Surface Free Energies of Solid Metals: Estimation from Liquid Surface Tension Measurements. *Surf. Sci.* **1977**, *62*, 267−276.
(47) Kittel, C. *Introduction to Solid State Physics*, 7th ed.; Wiley: New York, 1996.
(48) Djurisic, A. B.; Li, E. H. Modeling the Optical Constants of $CuGaSe_2$ and $CuInSe_2$. *Appl. Phys. A: Mater. Sci. Process.* **2001**, *73*, 189−192.
(49) Sarmiento-Pérez, R.; Botti, S.; Schnohr, C. S.; Lauermann, I.; Rubio, A.; Johnson, B. Local Versus Global Electronic Properties of Chalcopyrite Alloys: X-ray Absorption Spectroscopy and Ab Initio Calculations. *J. Appl. Phys.* **2014**, *116*, 093703.
(50) Gueymard, C. The Sun's Total and Spectral Irradiance for Solar Energy Applications and Solar Radiation Models. *Sol. Energy* **2004**, *76*, 423−453.
(51) Arndt, W.; Dittrich, H.; Schock, H. W. $CuGaSe_2$ Thin Films for Photovoltaic Applications. *Thin Solid Films* **1985**, *130*, 209−216.
(52) Hörig, W.; Neumann, H.; Sobotta, H.; Schumann, B.; Kühn, G. The Optical Properties of $CuInSe_2$ Thin Films. *Thin Solid Films* **1978**, *48*, 67−72.

DOI: 10.1021/acs.jpcc.5b07350
J. Phys. Chem. C 2015, 119, 22732−22736